# Adaptive suppression of smart jamming with FDA permutation

Asgeir Nysaeter
FFI(Norwegian Defence
Research Establishment)
Kjeller, Norway
Email: asgeir.nysater@ffi.no

***Abstract*—By adding a frequency increment to the carrier frequency of the pulses transmitted from an antenna array, it becomes possible to make the beam dependent on both frequency and range. This is called a frequency diverse array (FDA), and it is known that FDA can improve the system against both clutter and jamming. In this paper, it is shown by simulation, that suppression of the jammer is possible if the FDA increments are randomly permutated. If the jammer is not able to return the radar pulse within the pulse repetition interval (PRI), the radar will expect a return pulse with another FDA patteren in the next PRI. The idea has been tested by simulating a phased MIMO-FDA radar with an 8x2 antenna and four MIMO beams, and by processing the received signals with a recursive Capon estimator.**

## I. Introduction

Due to increased complexity and size reduction of electronic circuits, more functionality can be included in military systems. Smart jammers can be put into attacking missiles or air fighters, or into defending air, sea or ground platforms. The task is to confuse or deceive the adversary. As the jammer is programmed with more sophisticated algorithms, the more difficult it becomes to detect the jammer. Research on algorithms to reduce the effect of smart jammers is therefore an important task.

Signal processing using frequency diverse array (FDA) technique has been an area of active research since its introduction [1]. By using FDA, beamforming can be performed both in the angle and range domain. This is achieved by adding a small increment to the pulse carrier frequency, giving a transmitted wavefront that will bend as a function of distance. The benefits are more degrees of freedom and better possibility to attenuate unwanted interference. FDA has been combined with Multiple Input Multiple Output (MIMO) processing [2], [3], [4]. An even better possibility for unwanted interference suppression can be achieved by combining MIMO and FDA.

A smartjammer can try to hide real targets or generate virtual targets by returning a manipulated radar pulse. If the radar uses FDA technique, the jammer should respond from the searched angle-distance point to interfere with the radar response. This is explored for a MIMO-FDA radar in [5] as an aid for jamming suppression. In [6] the jammer plus noise covariance matrix is estimated based on nonhomogeneous sampling for jammer suppression, and in [7] jammers are suppressed in a MIMO-FDA radar based on unequal FDA frequency increments calculated by simulated annealing. Other papers treating jamming suppression with a MIMO/FDA radar are [8], [9].

This paper will show that jammers can be suppressed based on random permutation of the FDA increments. If the jammer wants to hide a target flying closer to the radar than the jammer, or flying together with the jammer, the jammer will probably not be able to respond within the angle-distance main lobe to the target if FDA is used. It must respond within the next PRI (pulse repetition interval). When the radar receives the echo pulse from the jammer, the FDA increments for the channel pulses have been permutated and another echo return FDA pattern is expected. Therefore, using FDA, the jammer will have reduced chance of destroying target tracks in the radar. Random FDA permutation can be used together with a fast recursive adaptive estimator to scan the angle-range space. The recursive Capon estimator simulated in the paper treats the random permutations as additional noise. In a modern, programmable and active phased array radar, both the FDA random permutation system and the recursive adaptive estimator can be implemented in firmware.

The simulations presented use the active X-band radar in Fig. 1 as a model [10], [11]. Two 8-channel TX/RX-boards and an 2x8 subantenna in the 8x8 phased array antenna are used. With FDA it will be able to search and track targets in the two-dimensional angle-distance space, not in the elevation space. Dividing the 2x8 antenna into four 2x2 antennas and using orthogonal codes between the subarray outputs, a phased MIMO radar is realized with a larger virtual receive array [12].

## II. Signal model for the FDA-MIMO radar

An active phased MIMO-FDA array radar as in Fig. 1 is assumed. The FDA frequency increment $\Delta f_m$ for each antenna channel is small relative to the carrier frequency and is permutated in a random way from pulse to pulse to attenuate

Dette er en postprint-versjon/This is a postprint version.
DOI til publisert versjon/DOI to published version: 10.1109/RadarConf2248738.2022.9764259

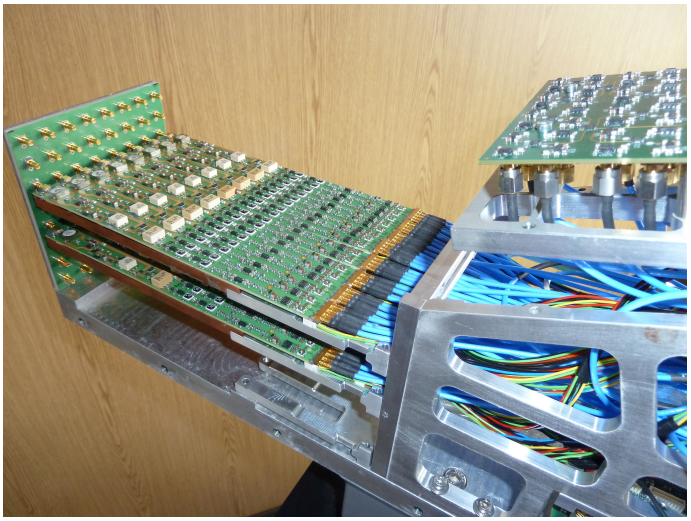

Fig. 1. The 2x8 antenna MIMO-FDA radar simulated in the paper.

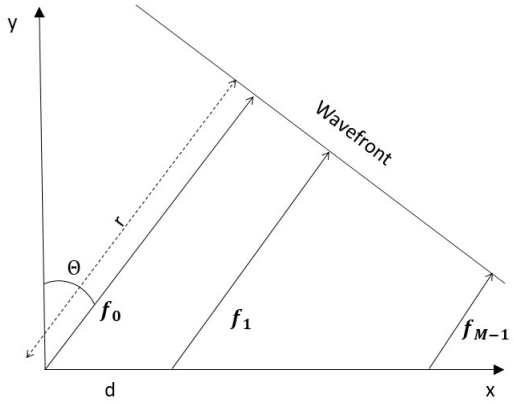


Fig. 2. FDA wavefront from the transmitting array.

a possible jammer disturbance. The pulse frequencies from the $M$ transmit antennas can be expressed as

$$\begin{aligned} f_m &= f_0 + \Delta f_m \\ \Delta f_m &\in [0, ..., M-1]\Delta f \qquad m = 0, ...., M-1 \end{aligned} \quad (1)$$

$f_0$ is the carrier frequency. Assuming a linear array with distance $d$ between the elements, at a distance $r$ from the reference element the phase difference between the pulse from the reference element and from element $m$ for a beam pointing in the direction $\theta$ becomes (Fig. 2)

$$\begin{aligned} \Delta\varphi_m &= -\frac{2\pi}{c}(f_0 + \Delta f_m)(r - d(m-1)\sin\theta) + \frac{2\pi}{c} f_0 r \\ &= -\frac{2\pi}{c}\Delta f_m r + \frac{2\pi}{c} f_0 d(m-1)\sin\theta + \frac{2\pi}{c}\Delta f_m d(m-1)\sin\theta \\ &\approx -\frac{2\pi}{c}\Delta f_m r + \frac{2\pi}{c} f_0 d(m-1)\sin\theta \end{aligned} \quad (2)$$

The first term is due to the frequency increment and shows that the phase difference depends on the distance to the target. The second term is equal to the array phase difference and the third term can be neglected. Thus adding small frequency differences to the carrier frequency makes the phase difference dependent on the target distance.

The n'th receiver input can be expressed as

$$\begin{aligned} y_n(t) &= \sum_{m=0}^{M-1} \beta_{mn} s_m(t - \tau_{mn}) \exp\left[j2\pi f_m(t - \tau_{mn})\right] + n_{mn} \\ &\approx \sum_{m=0}^{M-1} \beta_{mn} s_m(t - \tau_0) \exp\left[j2\pi f_m(t - \tau_{mn})\right] + n_{mn} \\ n &= 0, ..., N-1 \end{aligned} \quad (3)$$

$s_m(t)$ is the pulse from transmit antenna $m$, $\beta_{mn}$ is the complex target response, $\tau_{mn}$ is the propagation delay and $n_{mn}$ is the noise from transmit antenna $m$ to receive antenna $n$. Assuming a narrow band pulse $s_m(t - \tau_{mn}) \approx s_m(t - \tau_0)$ where $\tau_0 = \frac{2R_0}{c}$ is the common round trip delay. After down-conversion with $f_0$ and matched filtering, assuming orthogonal $s_m(t)$ pulses, the maximum value for pulse $m$ from a target at reference distance $R_0$ and azimuth angle $\theta_0$ in receiver $n$ becomes [7]

$$\begin{aligned} &y_n(R_0, \theta_0) = \\ &\sum_{k=0}^{M-1} \int_{\tau_0}^{\tau_0+T} \beta_{kn}[s_k(t-\tau_0)\exp\left[j2\pi f_k(t-\tau_{kn})\right] + n_{kn}] s_m^*(t-\tau_0) dt \approx \\ &\gamma_{mn} \exp\left[j2\pi(\Delta f_m \frac{-2R_0}{c} + \frac{f_m}{c}\mathbf{u}(\theta_0)\cdot\mathbf{d}_m + \frac{f_m}{c}\mathbf{u}(\theta_0)\cdot\mathbf{d}_n)\right] + n'_{mn} \\ &n = 0, ..., N-1, \quad m = 0, ..., M-1 \end{aligned} \quad (4)$$

$T$ is the pulse length, $\mathbf{u}(\theta_0)$ is a unit vector in direction $\theta_0$ and $\mathbf{d}_m$ is the vector from the array center to antenna $m$. $n'_{mn}$ is the noise term after matched filtering, and different constants have been put into the complex term $\gamma_{mn}$. The received signal vector can be expressed by ($\odot$ is the Hadamard product,$\otimes$ is the Kronecker product)

$$\mathbf{y}(R_0, \theta_0) = \boldsymbol{\gamma}_{mn} \odot ([\mathbf{a}(R_0) \odot \mathbf{a}(\theta_0)] \otimes \mathbf{b}(\theta_0)) + \mathbf{n}' \quad (5)$$

where

$$\begin{aligned} \boldsymbol{\gamma}_{mn} &= [\gamma_{0,0}, ..., \gamma_{M-1,0}, ..., \gamma_{M-1,N-1}]^T \\ \mathbf{a}(R_0) &= [e^{-j4\pi\Delta f_0 \frac{R_0}{c}}, ..., e^{-j4\pi\Delta f_{M-1}\frac{R_0}{c}}]^T \\ \mathbf{a}(\theta_0) &= [1, ..., e^{j2\pi\frac{f_{M-1}}{c}\mathbf{u}(\theta_0)\cdot\mathbf{d}_{M-1}}]^T \\ \mathbf{b}(\theta_0) &= [1, ..., e^{j2\pi\frac{2\pi f_{N-1}}{c}\mathbf{u}(\theta_0)\cdot\mathbf{d}_{N-1}}]^T \\ \mathbf{n}' &= [n'_{0,0}, ..., n'_{M-1,0}, ..., n'_{M-1,N-1}]^T \end{aligned} \quad (6)$$

If a jammer responds to the radar pulse, the jammer echo time delay will be the sum of the round trip delay, the time

Dette er en postprint-versjon/This is a postprint version.
DOI til publisert versjon/DOI to published version: 10.1109/RadarConf2248738.2022.9764259

used to process the signal in the jammer and a possible artificial delay made by the jammer [13]

$$\tau_j = \frac{2R_j}{c} + \tau_{processing} + \tau_{artificial} \quad (7)$$

Including the jammer response from the angle-distance pair $(R_j, \theta_j)$ in Eq. 5, the expression becomes

$$\mathbf{y}(R_0, \theta_0) = \gamma_{mn} \odot ([\mathbf{a}(R_0) \odot \mathbf{a}(\theta_0)] \otimes \mathbf{b}(\theta_0) + [\mathbf{a}(R_j) \odot \mathbf{a}(\theta_j)] \otimes \mathbf{b}(\theta_j)) + \mathbf{n}' \quad (8)$$

Since the radar in Fig. 1 is a phased MIMO radar with four 2x2 transmit antennas, few beams are needed to cover the angle-range area of interest. Fig. 3, 4 and 5 show the main transmit lobe. The 3 dB (range, azimuth) width is (3081.6 $m$, 79.5°) when $\Delta f = 30$ kHz.

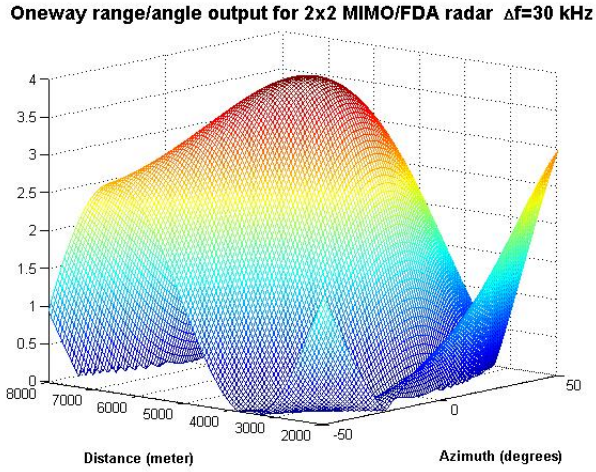


Fig. 3. 2x2 MIMO/FDA transmit pattern with $\Delta f = 30$ kHz.

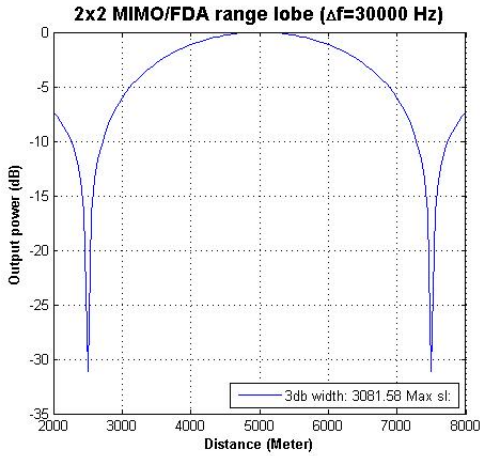


Fig. 4. 2x2 MIMO/FDA transmit distance pattern with $\Delta f = 30$ kHz.

## III. Recursive adaptive beamforming

Adaptive processing of the received response will increase the resolution of the main beam (angle-distance) lobe and help

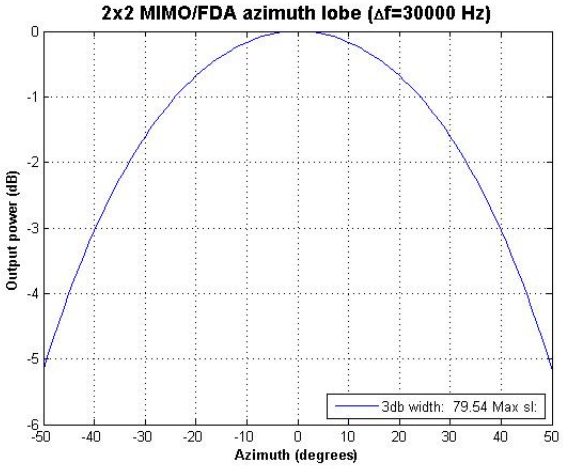


Fig. 5. 2x2 MIMO/FDA transmit azimuth pattern with $\Delta f = 30$ kHz.

suppressing unwanted interference. A well known adaptive algorithm is the Capon estimator [2]. The weight vector $\mathbf{w}(R, \theta)$ is calculated by minimizing the following expression

$$\min_{\mathbf{w}} \mathbf{w}^h(R,\theta) \hat{\mathbf{C}}_{\mathbf{yy}}(R,\theta) \mathbf{w}(R,\theta) \text{ subject to } \mathbf{w}^h(R,\theta)\mathbf{b}(R,\theta) = 1 \quad (9)$$

$\mathbf{b}(R, \theta)$ is the beam steering vector for point $(R, \theta)$. This means that we want unit response from the (angle-distance) search point, and minimum response from all other points. The sample covariance matrix $\hat{\mathbf{C}}_{\mathbf{yy}}(R, \theta)$ is calculated for each angle-distance pair by

$$\hat{\mathbf{C}}_{\mathbf{yy}}(R, \theta) = \frac{1}{2NM} \sum_{k=0}^{2NM-1} \mathbf{y}(t_{k-NM}, R, \theta) \mathbf{y}^h(t_{k-NM}, R, \theta) \quad (10)$$

Usually, twice the size of the receive signal vector is sufficient for a reliable estimate of the covariance matrix, according to Brennan's rule [2]. The constrained minimization expression in eq. 9 gives the optimum weight vector

$$\hat{\mathbf{w}}(R, \theta) = \frac{\hat{C}_{yy}^{-1}(R, \theta)\mathbf{b}(R, \theta)}{\mathbf{b}^h(R, \theta)\hat{C}_{yy}^{-1}(R, \theta)\mathbf{b}(R, \theta)} \quad (11)$$

The expression in equation 11 is usually too demanding to calculate in real time for each ( angle-distance) scan point. Instead a recursive estimator for $\mathbf{C}_{yy}^{-1}$ is used. By splitting a matrix $\mathbf{A}$ in four submatrices, the following rule for matrix inversion is used [14]

$$[\mathbf{A}_{11} - \mathbf{A}_{12}\mathbf{A}_{22}^{-1}\mathbf{A}_{21}]^{-1} = \mathbf{A}_{11}^{-1} + \mathbf{A}_{11}^{-1}\mathbf{A}_{12}[\mathbf{A}_{22} - \mathbf{A}_{21}\mathbf{A}_{11}^{-1}\mathbf{A}_{12}]^{-1}\mathbf{A}_{21}\mathbf{A}_{11}^{-1} \quad (12)$$

By using the recursive update formula for $\hat{\mathbf{C}}_{\mathbf{yy}}$

$$\hat{\mathbf{C}}_{\mathbf{yy}}(k) = (1-\alpha)\hat{\mathbf{C}}_{\mathbf{yy}}(k-1) + \alpha \mathbf{y}(k)\mathbf{y}^h(k) \quad 0 < \alpha < 1 \quad (13)$$

and first calculating

$$\mathbf{v}(k) = \hat{\mathbf{C}}_{yy}^{-1}(k-1)\mathbf{y}(k) \quad (14)$$

the update formula can be expressed as [15]

$$\hat{\mathbf{C}}_{yy}^{-1}(k) = \frac{1}{1-\alpha}\hat{\mathbf{C}}_{yy}^{-1}(k-1) - \frac{\alpha}{(1-\alpha)^2} \frac{\mathbf{v}(k)\mathbf{v}^h(k)}{1 + \frac{\alpha}{1-\alpha}\mathbf{y}^h(k)\mathbf{v}(k)} \quad (15)$$

Dette er en postprint-versjon/This is a postprint version.
DOI til publisert versjon/DOI to published version: 10.1109/RadarConf2248738.2022.9764259

Note that the Capon estimator is known to be sensitive to pointing errors and deviating target response. The FDA random permutations and possible pointing errors can help making the recursive estimator more robust.

## IV. Simulation results with random permutation of the freqency increments

The simulated MIMO-FDA radar with random permutation of the frequency increments has been tested on a target with speed 10 m/s following an ellipsoid path. The search space has been divided in a grid with resolution $0.2°, 25\ m$, and the response has been processed with the recursive Capon estimator. The jammer has returned echos with equal power to the target, and the jammer response with wrong frequency increments relative to the transmitted ones has been compared to the target response with correct increments.

Fig. 6 shows the beamforming response when random permutation of the FDA frequency increments has been used. The response of beam no. 1 has correct FDA increments. As can be seen, the response is heavily weakened when the the permutation does not match.

The inverse Capon update constant $\alpha$ has been set to 0.05, and using the 2x8 antenna in Fig. 1, 4 MIMO beams gives a virtual receive antenna with 64 elements. $\Delta f$ has been set to 30 kHz and $f_0$ to 8.25 GHz. Fig. 7 shows the Capon track estimates (in red) of the target path (in black). Jammer location is shown in green. The jammer location is (2667,6667), and the target start location is (2000,6000). As can be seen, the jammer has little effect on the target track. Fig. 8 and Fig. 9 show the track status after 60 iterations. The jammer effect has almost been removed. In contrast, the jammer response is approximately equal to the target response in Fig. 10 when a fixed frequency increment without random permutation is used.

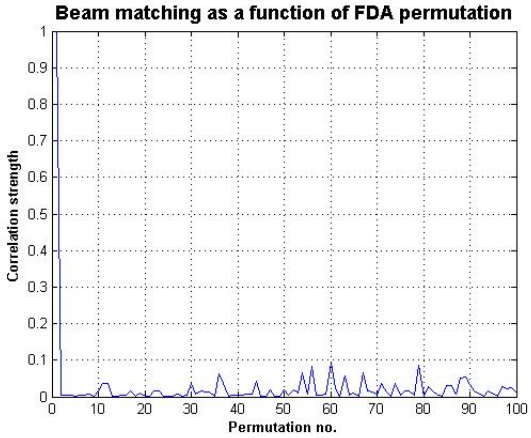


Fig. 6. Beamforming response with FDA permutation.

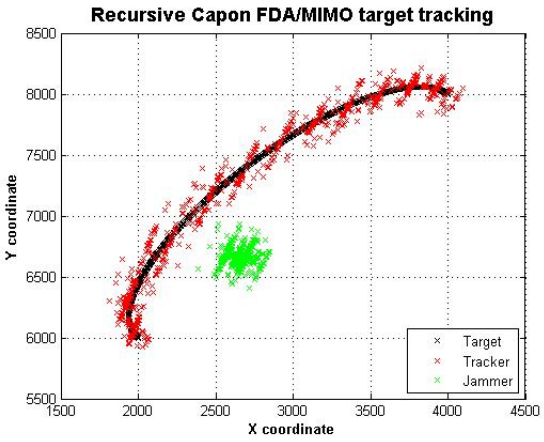


Fig. 7. Recursive Capon target track using 4 beam MIMO/FDA radar with random FDA permutations.

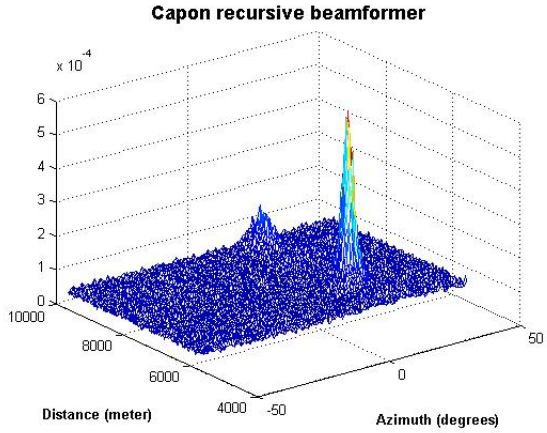


Fig. 8. Track status after 60 iterations.

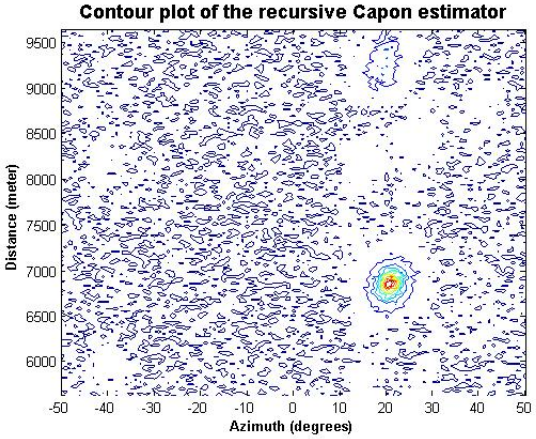


Fig. 9. Contour plot of track status after 60 iterations.

## V. Conclusion

Using FDA radar the jammer should respond within the angle-distance main lobe of the target to make maximum disturbance on the track, in contrast to a non-FDA radar where it is sufficient to respond within the angle main lobe. In addition, if the jammer is not able to respond within the current PRI of the radar, more jammer suppression can be achieved by using random FDA permutation. For optimum suppression through

Dette er en postprint-versjon/This is a postprint version.
DOI til publisert versjon/DOI to published version: 10.1109/RadarConf2248738.2022.9764259

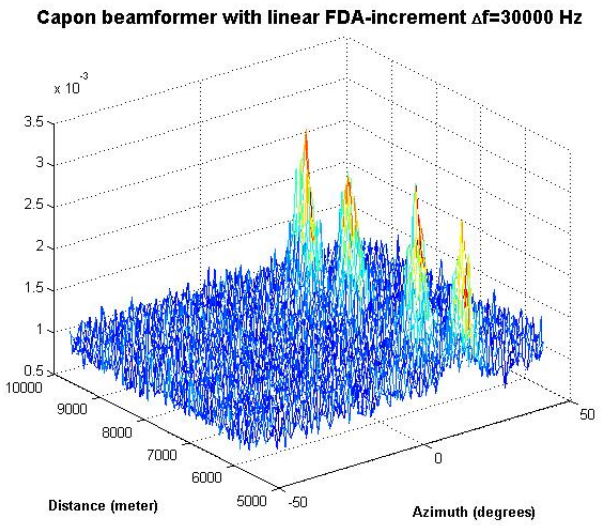


Fig. 10. Track status with linear FDA increments.

FDA permutation, different random permutation sequences should be tested with regard to the used radar and radar parameters. The recursive Capon estimator is a fast algorithm for adaptive scanning of the angle-range space, and it can be used together with the FDA permutations.

## REFERENCES


[1] P. Antonik and M. C. Wicks, "Frequency Diverse Array Radars," in *Proc. IEEE Radar Conference*, Verona, NY, Apr. 24-27 2006.

[2] J. Li and P. Stoica, MIMO Radar Signal Processing, John Wiley & Sons, 2009.

[3] P.,F. Sammartino, C. J. Baker, H. D. Griffiths, "Frequency Diverse MIMO Techniques for Radar," *IEEE Transactions on Aerospace and Electronic Systems*, Vol. 49., No. 1, Jan. 2013.

[4] W.-Q. Wang, "Phased-MIMO Radar With Frequency Diversity for Range-Dependent Beamforming," *IEEE Sensors Journal*, Vol. 13., No. 4, Apr. 2013.

[5] J. Xu, G. Liao, S. Zhu, H. C. So,"Deceptive jamming suppression with frequency diverse MIMO radar," *Signal Processing*, No. 113, March 2015.

[6] L. Lan, G. Liao, J. Xu,Y. Zhang, F. Fioranelli "Suppression Approach to Main-Beam Deceptive Jamming in FDA-MIMO Radar Using Nonhomogeneous Sample Detection," *IEEE Access*, Vol. 6., No. 3, June 2018.

[7] Y. Wang, S. Zhu, "Main-Beam Range Deceptive Jamming Suppression With Simulated Annealng FDA-MIMO Radar," *IEEE Sensors Journal*, Vol. 20., No. 16, Aug. 2020.

[8] J. Xu, J. Kang, G. Liao, "Mainlobe Deceptive Jammer Suppression with FDA-MIMO Radar," *IEEE 10th Sensor Array and Multichannel Signal Processing Workshop (SAM)*, 2018.

[9] L. Lan, J. Xu, G. Liao, Y. Zhang, F. Fioranelli, H. C. So, "Suppression of Mainbeam Deceptive Jammer With FDA-MIMO Radar," *IEEE Transactions on Vehicular Technology*, Vol. 69., No. 10, Oct 2020.

[10] F. Gulbrandsen, A. Nysaeter, Y. Paichard, "Design of Wide-angle Scan, X-band, Digital Array Radar Antenna," in Proc. *IEEE Radar Conference*, 2014.

[11] H. Iwe, O. Opland, J. R. Nilssen, F. Gulbrandsen, A. Nysaeter, "Packaging and cooling of an X-band digital array radar T/R module," in Proc. *IEEE Radar Conference*, 2017.

[12] A. Hassanien and S. A. Vorobyov, "Phased-MIMO Radar: A Tradeof Between Phased-Array and MIMO Radars," *IEEE Transactions on Signal Processing*, June 2010.

[13] G. F. Stott, "Digital Modulation for Radar Jamming," *IEE Colloquium on Signal Processing in Electronic Warfare*,Jan. 1994.

[14] F. C. Schweppe, Uncertain Dynamic Systems, Prentice-Hall, Inc., Englewood Cliffs, New Jersey, 1973.

[15] C. A. Baird, Jr. and J. T. Rickard, "Recursive Estimation in Array Processing," *Proceedings of the Fifth Asilomar Conference on Circuits and Systems*, Pacific Grove, CA, pp. 509-513, 1971.



Dette er en postprint-versjon/This is a postprint version.
DOI til publisert versjon/DOI to published version: 10.1109/RadarConf2248738.2022.9764259